



Contents lists available at ScienceDirect

Behavioural Brain Research

journal homepage: www.elsevier.com/locate/bbr

Research report

Subtle behavioral changes and increased prefrontal-hippocampal network synchronicity in APP^{NL-G-F} mice before prominent plaque depositionAmira Latif Hernandez^{a,1}, Disha Shah^{b,1}, Kathleen Craessaerts^c, Takaomi Saido^d, Takashi Saito^d, Bart De Strooper^c, Annemie Van der Linden^b, Rudi D'Hooge^{a,*}^a Laboratory of Biological Psychology, University of Leuven, KU Leuven, Belgium^b Bio-Imaging Lab, University of Antwerp, Belgium^c VIB center for the biology of disease, KU Leuven, Belgium^d Laboratory for Proteolytic Neuroscience, Riken Brain Science Institute, Japan

ARTICLE INFO

Keywords:

Alzheimer's disease
Knock-in mouse models
Behavioral assessment
Amyloid
Resting state fMRI

ABSTRACT

Amyloid- β (A β) peptides occur in the brains of patients with Alzheimer's disease (AD), but their role in functional impairment is still debated. High levels of APP and APP fragments in mice that overexpress APP might confound their use in preclinical research. We examined the occurrence of behavioral, cognitive and neuroimaging changes in APP^{NL-G-F} knock-in mice that display A β 42 amyloidosis in the absence of APP overexpression. Female APP^{NL-G-F} mice (carrying Swedish, Iberian and Arctic APP mutations) were compared to APP^{NL} mice (APP Swedish) at 3, 7 and 10 months. Mice were subjected to a test battery that referred to clinical AD symptoms, comprising cage activity, open field, elevated plus maze, social preference and novelty test, and spatial learning, reversal learning and spatial reference memory performance. Our assessment confirmed that behavior at these early ages was largely unaffected in these mice in accordance with previous reports, with some subtle behavioral changes, mainly in social and anxiety-related test performance. Resting-state functional MRI (rsfMRI) assessed connectivity between hippocampal and prefrontal regions with an established role in flexibility, learning and memory. Increased prefrontal-hippocampal network synchronicity was found in 3-month-old APP^{NL-G-F} mice. These functional changes occurred before prominent amyloid plaque deposition.

1. Introduction

Alzheimer's disease (AD) is characterized by the progressive brain deposition of extracellular 40–42 residue amyloid- β peptide (A β) [1–3], and neurofibrillary tangles [4]. Transgenic mice overexpressing APP and Tau have been instrumental to recent AD research, but these mice may have artificial phenotypes because they overproduce APP fragments [5,6]. Models that endogenously overproduce A β 42 without overexpressing APP have been generated by knock-in (KI) of a humanized A β sequence [7]. Characterization of the functional consequences of the KI strategy on complex behavioral and cognitive abilities and brain circuitry is still limited, and previous reports showed only mild behavioral defects at the age examined in the present report [8].

Patients that are eventually diagnosed with clinical AD show problems in executive functioning and attention at early stages of the disease [9]. The present study evaluates the validity of APP knock-in (KI) mice as models of clinical AD. APP^{NL-G-F} mice carrying Iberian and Arctic mutations in the A β sequence were compared to APP^{NL} mice

carrying only the Swedish mutation to dissociate the effects of aggressive A β pathology. We investigated these mice using behavioral tasks that assess higher-order functions (such as cognitive flexibility), which relate to defects observed in AD patients [10–12]. Behavioral flexibility is required when faced with environmental changes, which starts declining in early phases of AD pathology. Behavioral assessment and reversal learning included in the present study models neuropsychological testing in patients [13–17]. In addition, resting-state functional MRI (rsfMRI) was used as a non-invasive imaging method, based on fluctuations in blood oxygen level-dependent (BOLD) signals [18], to assess connectivity between cortical regions and brain network integrity [19]. Measuring fMRI during the brain's resting state has been used to define early disease biomarkers, since changes in connectivity underlie different neuropsychiatric disorders [19,20], and rsfMRI is a clinically feasible tool for early diagnosis [21].

* Corresponding author at: Laboratory of Biological Psychology, KU Leuven, Tiensestraat 102, 3000 Leuven, Belgium.

E-mail address: rudi.dhooge@kuleuven.be (R. D'Hooge).¹ Equal contribution.<https://doi.org/10.1016/j.bbr.2017.11.017>

Received 17 October 2017; Received in revised form 14 November 2017; Accepted 16 November 2017

0166-4328/ © 2017 Elsevier B.V. All rights reserved.

2. Methods

2.1. Animals

APP^{NL} and APP^{NL-G-F} mice were derived from the Riken Institute colony (Japan). APP^{NL-G-F} mice co-express Swedish (KM670/671NL), Beyreuther/Iberian (I716F) and Arctic (E693G) mutations, whereas APP^{NL} mice only express the Swedish mutation and were used as controls in all tests performed. The behavioral test battery was carried out in homozygous female mice aged of 3, 6 and 10 months old. There were 14 APP^{NL} and 14 APP^{NL-G-F} mice in the 3-month-old group, 8 APP^{NL} and 8 APP^{NL-G-F} mice in the 6-month-old group, and 12 APP^{NL} and 12 APP^{NL-G-F} mice in the 10-month-old group. Saito and colleagues observed age-dependent A β amyloidosis in homozygous APP^{NL-G-F} mice. Notably, cortical deposition began by 2 months and was saturated from around 7 months.

2.2. Immunostaining

The amyloid plaque load was measured in brain sagittal vibratome sections (60 μ m) from mice transcardially perfused with PFA. The sections were stained for amyloid plaques using immunofluorescence with an A β primary antibody (6E10, against A β ₁₋₁₇, Sigma) after antigen retrieval in sodium citrate buffer. Antibody-antigen complexes were revealed using a DyLight 650-conjugated goat anti mouse secondary antibody. DAPI (4',6-diamidino-2-phenylindole) (Invitrogen) was used as counterstain. Digital images were taken on a Nikon A1R Eclipse Ti microscope.

2.3. Cage and exploratory activity assessment

Mice were placed in small animal cages between 3 infrared beams to monitor 23 h spontaneous activity as previously described [22]. After 15 min habituation, registration of beam crossings started at 4pm with lights being switched off at 8pm (12 h on/off cycle). Open field (OF) locomotor behavior was monitored in observation areas with walls and floor consisting of transparent PVC ($w \times d \times h$: 50 \times 50 \times 30 cm), and placed on translucent shelves inside an isolation cabinet. Indirect lighting was applied from underneath the setups. Cameras mounted above the arenas transmitted images to computers equipped with ANYMAZE™ video tracking software (Stoelting Co., IL, USA). Animals were placed in the left corner of the OF arena proximal to the experimenter and allowed to explore the open arena freely for 1 h. The arena was cleaned between animals with a dry towel. The open field was virtually divided into three different zones: an outer periphery (0–5 cm from OF walls), inner periphery (5–10 cm from OF walls) and center square. Exploration parameters such as distance travelled, time spent and number of entries were analyzed for 10 min.

Anxiety-related exploration was evaluated in the elevated plus maze (EPM) as described before [22]. Briefly, the EPM comprised two arms (5 cm wide, 20 cm long, elevated 40 cm above table top) closed by side walls, and two arms without walls. Mice were placed at the center of the maze, and were allowed to explore freely for 11 min (1 min habituation and 10 min recording). Exploratory activity was recorded by 5 IR beams (4 for arm entries, and 1 for open arm dwell) connected to a computerized activity logger.

2.4. Sociability/preference for social novelty task

A social novelty and recognition task was adapted from Nadler and colleagues (2004) as described in detail elsewhere [23]. Setup consisted of a rectangular transparent Plexiglas box ($w \times d \times h$: 94 \times 28 \times 30 cm) divided into three chambers. Mice could circulate between left, right (29 \times 28 \times 30 cm) and central chamber (36 \times 28 \times 30 cm) via openings ($w \times h$: 6 \times 8 cm) in division walls between chambers. Openings could be manually closed to limit access

to chambers. The setup had an opaque floor and was illuminated indirectly from underneath the setup. It was placed inside an enclosure to limit environmental distractions. Two cameras were located 60 cm above the setup and ANY-maze™ Video Tracking System software (Stoelting Co., IL, USA) was used to record and analyze movements of animals. Cylindrical wire cups (height \times diameter: 11 \times 12 cm) that contained stranger mice were placed in the left and right chamber. The procedure consisted on three consecutive phases, between the phases the animal was maintained in the middle compartment. During the first phase (acclimation phase) mice were habituated to the apparatus and placed in the middle chamber with both divider doors closed and left to explore for 5 min. During this trial, empty wire cages were present in left and right chambers visible from the middle chamber. In the second phase (sociability phase) one stranger mouse (S1) was placed in wire cage in either left or right chamber, the other wire cage was left empty. Exploratory behavior (exploring and sniffing) towards S1 and the empty cage was recorded for 10 min. Finally during the third phase (social recognition phase) a second stranger mouse (S2) was placed in empty wire cage with S1 mouse remaining in its cage. Exploratory behavior towards S1 and S2 was again recorded for 10 min. We calculated preference ratio (Ratio_{Pref}) as Time_{S1}/(Time_{S1} + Time_{empty}), and recognition ratio (Ratio_{Rec}) as Time_{S2}/(Time_{S1} + Time_{S2}). The position of S1 and S2 was counterbalanced between animals. The setup was thoroughly cleaned with water and paper towel between animals. At the end of each testing day, test setup was cleaned with 30% ethanol. Stranger mice were 3-month old, group-housed (2 per cage) female C57BL/6J mice that had served as stranger mice in other SPSN experiments before. Distance travelled in each chamber was also calculated.

2.5. Morris water maze performance

Spatial memory was assessed in the Morris water maze (MWM) [24], using a training protocol adapted for mice [25]. The maze had a diameter of 150 cm and contained water (23 °C) that was made opaque with non-toxic white paint. The pool was located in a brightly lit room with distal visual cues, including computer, tables and posters with geometric figures attached to the walls. Images were recorded with a PC-interfaced camera located above the water maze and analyzed with EthoVision software (Noldus, Wageningen, The Netherlands). During acquisition trials, a small platform (diameter 15 cm) was hidden beneath the surface at a fixed position. Mice were placed in the water at the border of the maze and had to reach the platform after which they were transported back to their home cage. Mice that did not reach the platform within 2 min were gently guided towards the platform and were left on it for 10 s before being placed back in their cages. Four of such daily training trials (inter trial interval: 15–30 min) were given on 5 subsequent days (Monday to Friday; acquisition days 1–5); the week after the same procedure was repeated (acquisition days 6–10). Data were averaged per trial day. Starting positions in the pool varied between four fixed positions (0°, 90°, 180° and 270°) so that on every training day, each position was used. The 4 starting positions define 4 quadrants: (i) the target quadrant where the escape platform is placed, (ii) the opposite quadrant which is at the opposite side of the target quadrant, (iii) the first adjacent quadrant and (iv) the second adjacent quadrant. During intertrial intervals, mice were placed under IR lamps to dry. Two probe trials were interspersed with training trials: probe 1 before start of training trials on acquisition day 6; probe 2 was run on the third day after acquisition day 11. During probe trials, the platform was removed from the pool and mice were allowed 100 s to search for the platform. This way, it could be verified whether mice showed a preference for the area where the platform used to be hidden. After acquisition trials, 3 daily reversal trials were performed on 5 subsequent days. The reversal phase consisted on placing the platform to the opposite quadrant.

2.6. Resting state magnetic resonance imaging

MRI acquisition and imaging data analyses was done as previously described in [26]. Briefly, resting-state imaging (rsfMRI) was performed on a 9.4T Biospec MRI system (Bruker BioSpin, Germany) with ParaVision 5.1 software (www.bruker.com). Three orthogonal multi-slice Turbo RARE T2-weighted images were acquired to allow uniform slice positioning (repetition time 2000 ms, echo time 15 ms, 16 slices of 0.4 mm). Field maps were acquired for each animal to assess field homogeneity, followed by local shimming, which corrects for inhomogeneity in a rectangular brain VOI. Resting-state signals were measured during a T2*-weighted single shot EPI sequence (repetition time 2000 ms, echo time 15 ms, 16 slices of 0.4 mm, 150 repetitions). Analysis consisted of two major steps. First, seed-based analysis was performed using right prefrontal cortex as seed region. A statistical difference map was obtained showing all voxels that were significantly different between the two groups (i.e., voxels that show differential FC with the right prefrontal cortex between sham and lesioned animals). This difference map was shown as an overlay on the EPI template. Next, the REST toolbox was used to compute z-transformed FC matrices for each subject using cortical regions that had shown different FC between the groups during seed-based analysis (i.e., prefrontal cortex, motor cortex, cingulate and retrosplenial cortex, somatosensory cortex, hippocampal CA1 region and thalamus). The time course of BOLD signals were extracted for each of these regions, and z-transformed correlation coefficients between time traces of each region pair were calculated and represented in a correlation matrix. Additionally, these matrices were used to calculate FC strength for each cortical region (i.e., mean strength of the correlation between a specific region and all other regions in the matrix). In the present study, the size of each group was as follows: 3 months APP^{NL} (n = 10), and APP^{NL-G-F} (n = 12); 6 months APP^{NL} (n = 10), and APP^{NL-G-F} (n = 10); 11 months APP^{NL} (n = 11), and APP^{NL-G-F} (n = 12).

2.7. Statistics

For behavioral tests, all data are shown as means \pm SEM. Differences between mean values were determined using 1-way or 2-way analysis of variance (ANOVA), or 2-way repeated measures (RM) ANOVA procedures with Tukey tests for post hoc comparison. ANOVA on the probe trial results used factors group and quadrant. In all statistical tests, differences of $p < 0.05$ were considered significant.

3. Results

3.1. A β plaques in brains of APP^{NL-G-F} and APP^{NL} mice

Antibodies to the N and C termini appeared to bind to both A β species in a similar manner. Using a combination of antibodies, we observed A β amyloidosis in APP^{NL-G-F} mice in an age dependent manner. We also observed early accumulation of A β plaques starting at the age of 2-2.5 months with full-blown pathology by 6 months in the cortex and hippocampus of APP^{NL-G-F} mice. In brains of APP^{NL} mice, we did not observe any plaques at the time points tested (Fig. 1).

3.2. Cage activity and exploration

APP^{NL} and APP^{NL-G-F} mice were tested in the cage activity device to investigate spontaneous activity of these mice. Over a 23-h period, the spontaneous activity of 3-month-old APP^{NL-G-F} mice (Fig. 2A, left panel) was significantly higher than the activity of APP^{NL} mice (RM-ANOVA: $F_{1,1170} = 11.56$; $p = 0.002$). However, this difference was not measured at 6 months (Fig. 2A, middle panel), and 10-month-old APP^{NL-G-F} mice (Fig. 2A, right panel) showed significantly increased overall activity across the 23 h period (RM-ANOVA: $F_{1,1034} = 6.406$; $p = 0.019$). Marked activity changes occurred between 8pm (after

lights were switched off) and 9 am (RM-ANOVA: $F_{22,506} = 9.682$; $p = 0.005$).

The open field task was used to investigate anxiety-related exploratory activity in APP^{NL} and APP^{NL-G-F} mice. In other AD mouse models, this test already highlighted anxiety and exploration disturbances [27]. In the open field test, the time spent in the arena center is a parameter that reflects anxiety, whereas total distance moved represents exploratory activity. As depicted in Fig. 2 B (right panel), 6-month-old APP^{NL-G-F} mice spent significantly more time in the arena center compared to APP^{NL} mice ($t = 2.818$; $p = 0.0258$). This increase of time spent in arena center indicates decreased anxiety, which is consistent with anxiolytic behavior in other AD mouse models [27,28]. Moreover, no differences were found in APP^{NL-G-F} mice exploration compared to APP^{NL} mice in the other age groups (Fig. 2B, right panel). In addition, we found that the total distance moved was consistently reduced in APP^{NL-G-F} mice (Fig. 2B, left panel), but not significantly between groups. A study performed in wild-type C57BL/6 mice [29] has shown that performance in the open field task is affected by increasing age. For example, Shoji et al. showed that subjects in older age groups travelled shorter distances than those in younger age groups [29]. The difference in time spent in arena center and distance moved found between younger and older APP^{NL} and APP^{NL-G-F} mice seem, therefore, to be an effect of ageing, unrelated to their AD pathology.

The elevated plus maze test allows evaluation of anxiety-related behaviors, since increased or decreased exploration of the open arms can indicate anxiolytic or anxiogenic behavior, respectively [28]. At 3 months of age (Fig. 3 left panel), the number of entries in the open arms (defined as number of beam crossings) was significantly increased in APP^{NL-G-F} mice (crossings: 30 ± 5 , $n = 7$) compared to APP^{NL} mice (crossings: 45 ± 4 , $n = 8$), whereas APP^{NL-G-F} entered the closed arm less frequently (81 ± 7) than APP^{NL} mice (99 ± 11). Non parametric t -test with Welch's corrections indicated a significant difference in the number of beam breaks between the two genotypes ($t = 2.53$; $p = 0.0297$), which is consistent with the anxiolytic behavior in other AD mouse models, likely induced by disinhibition resulting from AD pathology [27,28]. This decreased anxiety was obvious during the open field test as well (see above). At a later time point (6 months; Fig. 3, middle panel), APP^{NL-G-F} mice entered the open arms 46 ± 7 times, and the closed arm 76 ± 5 times, whereas APP^{NL} mice entered the closed arm 126 ± 8 , and the open arm 27 ± 3 times. RM-ANOVA confirmed the different preference of APP^{NL-G-F} mice for the open versus closed arms: a main effect of arm (open v. closed) on number of beam breaks was found ($F_{1,13} = 146$, $p < 0.0001$), a main effect of genotype ($F_{1,13} = 4.8$, $p = 0.0464$) and a genotype by arm interaction effect ($F_{1,13} = 42$, $p < 0.0001$). Indeed, t -test with Welch's correction indicated a significant difference in the number of beam breaks in the open arm between the two genotypes ($t = 2.456$; $p = 0.0396$). Surprisingly, APP^{NL-G-F} mice displayed a significant reduction in the number of entries in the closed arm compared to APP^{NL} ($t = 5.114$; $p = 0.0003$). At 10 months (Fig. 3, right panel), both groups visit the open arm equally often, whereas the close arms are significantly less visited by the APP^{NL-G-F} mice ($t = 2.593$; $p = 0.0223$). It should be noted in this respect that old C57BL/6 mice have been shown to exhibit a significantly higher percentage of open arm entries compared to younger animals [29].

3.3. Sociability and social recognition behaviors

Social memory was assessed in APP^{NL} and APP^{NL-G-F} mice by means of the Social Preference Social Novelty (SPSN) test. Social recognition was found to be impaired in several AD mouse lines [30,31]. During social preference (Fig. 4B) and recognition phases (Fig. 4C), statistical comparison of the data sets with an unpaired t -test (Welch's correction two-tailed) revealed no significant differences between the two groups at any of the ages tested (neither Ratio_{Pref}, nor Ratio_{Rec}). However, during the social preference trial, 10 months-old APP^{NL-G-F}

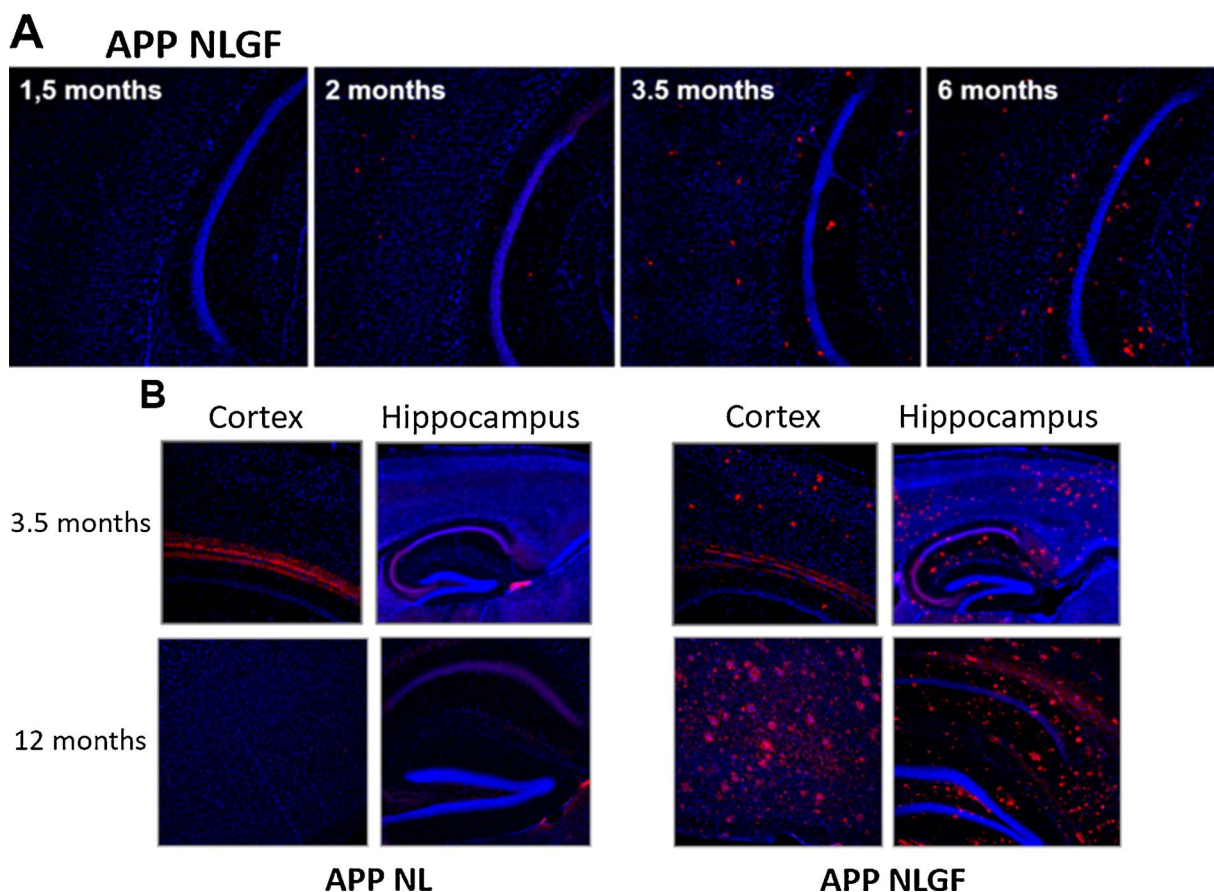


Fig. 1. A β deposition in APP^{NL} and APP^{NL-G-F} brains. (A) Brain sections from 1.5, 2, 3.5 and 6-month-old mice were immunostained using an A β_{42} antibody. Cortical and hippocampal immunoreactive amyloid plaque load were measured using confocal microscopy revealing amyloid plaques already at the age of 3.5 months, although very minor compared to 6-month-old APP^{NL-G-F} mice (n = 7, 10, 5 and 6 mice per indicated time point, respectively). (B) absence of amyloid plaques in neocortex and hippocampus of APP^{NL} mice (left) in contrast to APP^{NL-G-F} mice, at 3.5 and 12 months of age (APP^{NL}: n = 14, APP^{NL-G-F}: n = 16 at 12 months).

mice exhibited a reduced Ratio_{Pref} compared to APP^{NL}. APP^{NL-G-F} mice showed a non-significant reduction in Ratio_{Rec} during the recognition trial at 3, 6 and 10 months, which suggests that these mice display some mild social impairment. To investigate this further, time spent in the small periphery (closer to S1 or S2) was analyzed in both phases for every group at 3 (Fig. 4A, left panel), 6 (Fig. 4A, middle panel) and 10 months of age (Fig. 4A, right panel). RM-ANOVA of social preference trial indicated a main effects of *arena side* at 3 months ($F_{(1,15)} = 28.02$; $p < 0.0001$). Fig. 4A (left panel) shows that both groups prefer to approach mouse S1 to an empty cage, APP^{NL-G-F} to a higher degree than APP^{NL} mice. At 6 months, we found a similar effect of *stranger side* ($F_{(1,13)} = 7.203$; $p = 0.0188$), but the preference of APP^{NL-G-F} mice for S1 over the empty side is much smaller than at 3 months, possibly due to increased variability at this age.

Ten-month-old APP^{NL-G-F} mice display increased preference for the empty side over the S1, with a “*stranger side*” \times “*genotype*” interaction effect ($F_{(1,16)} = 5.044$; $p = 0.0392$). In the second trial, during the recognition phase, main effect of *stranger side* was present at 3 months ($F_{(1,15)} = 11.24$; $p = 0.0044$) and at 6 months of age ($F_{(1,13)} = 41.79$; $p < 0.0001$), whereas no effect was found at 10 months. In fact, as displayed in Fig. 4E, there is no preference in none of the groups towards S2 over S1. There is a tendency indicating that APP^{NL-G-F} mice explore the novel S2 mouse less than the known S1, although the difference is not significant. The fact that 10-month-old APP^{NL-G-F} displayed no interest in exploring S1 during the social preference trials might have influenced their performance in the social recognition trials.

To further investigate exploration patterns at 10 months, exploration time was analyzed in subsequent time bins of 2 min each per genotype condition and SPSN trial (Fig. 4D–G). During the social

preference trial, APP^{NL} mice showed preference for S1 over the empty side only during the first two time bins: RM-ANOVA indicated no effect of *stranger side* or *time bin* (Fig. 4D). Once they have explored S1, from time bin 3 they spend equal time in the empty side and S1 side. However, APP^{NL-G-F} mice (Fig. 4F) do not show any preference at all for the S1 during the time bin 1. On the contrary, from time bin two, they spent almost significantly more time in the empty side than with S1 ($t = 2.023$; $p = 0.0641$). This decreased interest for S1 persisted through the end of the trial (bins 3, 4 and 5), with a clear overall preference for the empty side (Fig. 4F). During the recognition trial, the control animals show a preference for S2 over S1 only during the first time bins (Fig. 4E), spending more time with the familiar mouse from time bin 3: RM-ANOVA indicated a main effect of *time bin* and *stranger side* interaction ($F_{(4,56)} = 3.585$; $p = 0.0113$). Interestingly, APP^{NL-G-F} mice showed slightly increased preference for S2 over S1 during the first time bin (Fig. 4G), with a strong preference for the familiar mouse (S1) over the novel one (S2) through the next 4 time bins (RM-ANOVA did not indicate significant effects). In summary, APP^{NL} mice showed pronounced sociability and preference for social novelty, especially during the first time bins, whereas such behavior was less pronounced or absent in APP^{NL-G-F} mice.

3.4. Spatial learning and memory

APP^{NL} and APP^{NL-G-F} mice were trained for 10 days to find the hidden platform in a large circular pool filled with opaque water in order to investigate spatial learning and memory as well as reversal learning. Probe trials were interspersed on day 6 and 11 after acquisition learning, and on day 6 after reversal learning to evaluate reference

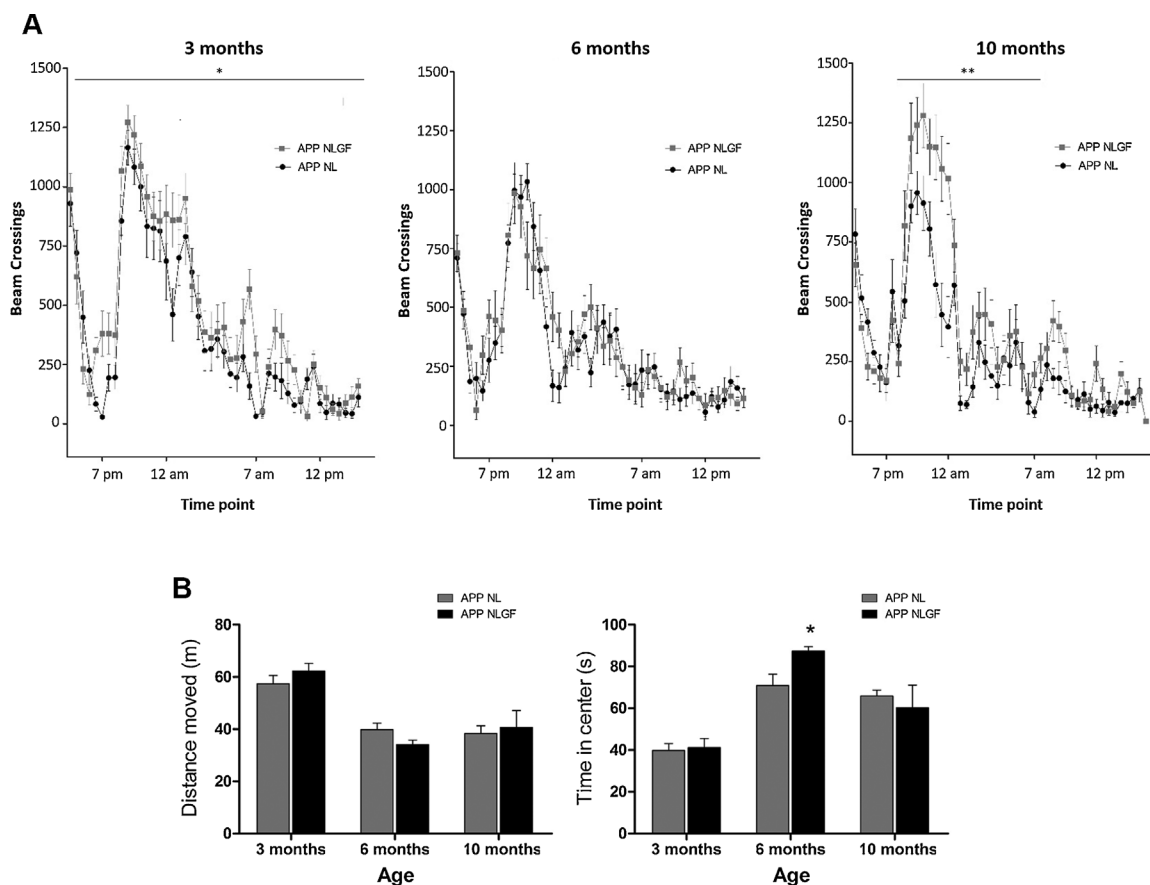


Fig. 2. Locomotor activity at 3, 6 and 10 months. (A) 23 h activity patterns in APP^{NL} (black circles) and APP^{NL-G-F} mice (grey squares), 3-month-old APP^{NL-G-F} mice (left panel, n = 14) display increased locomotor activity compared to APP^{NL} mice (n = 14); APP^{NL-G-F} (middle panel, n = 14) and APP^{NL} mice (n = 14) at 6 months; APP^{NL-G-F} (right panel, n = 11) and APP^{NL} mice (n = 13) at 10 months. See text for statistics. (B) Overall activity measures in APP^{NL-G-F} (black bars) and APP^{NL} mice (grey bars) in the open field. Left panel: at 3, 6 and 10 months of age, APP^{NL-G-F} mice (n = 14, n = 7, n = 12, respectively) travelled equal distances as APP^{NL} mice (n = 14, n = 8, n = 12, respectively); right panel: more anxiety-like behavior at 6 months in APP^{NL-G-F} (n = 7) compared to APP^{NL} mice (n = 7; see text for statistical analysis). No differences at 3 months, nor at 10 months between APP^{NL-G-F} (n = 13, n = 11, respectively) and APP^{NL} mice (n = 13, n = 11, respectively). Data are means \pm SEM.

memory. The latter is used as a paradigm to study cognitive flexibility, commonly known as the ability to change behavior in response to changes in the environment [32]. Other AD mouse models have shown impairments in spatial and reversal learning [33]. A learning curve was obtained by plotting the path length to find the platform on each training day. During the acquisition phase, 3–4 month-old APP^{NL-G-F} and APP^{NL} mice learned the platform position at a different rate ($F_{1,207} = 4.798$; $p = 0.04$), but there was no main effect of *day* and *group* interaction ($F_{9,207} = 0.7290$; $p = 0.7$; Fig. 5A). Thus, APP^{NL} mice were slower than APP^{NL-G-F} during the first days of training. However, post-hoc comparisons using the Tukey HSD test during the second probe indicated that APP^{NL} mice showed more pronounced target

quadrant preference ($p = 0.0182$) than their APP^{NL-G-F} littermates ($p = 0.2036$). As depicted in Fig. 5B, during probe 1, none of the groups displayed any preference for the target quadrant yet. Interestingly, at 6–7 months of age (Fig. 5B), APP^{NL-G-F} and APP^{NL} mice performed equally well during 10 days acquisition learning in the MWM. Repeated measures (RM) ANOVA of the acquisition phase for factor day indicated that all animals learned to locate the hidden platform ($F_{9,117} = 123.77$, $p < 0.001$). Reference memory performance was tested in probe trials 1 and 2, which indicated that both groups developed a preference for the target quadrant. Particularly, Tukey post-hoc comparisons during probe 2 showed that APP^{NL} as well as APP^{NL-G-F} mice spent significantly more time searching the target

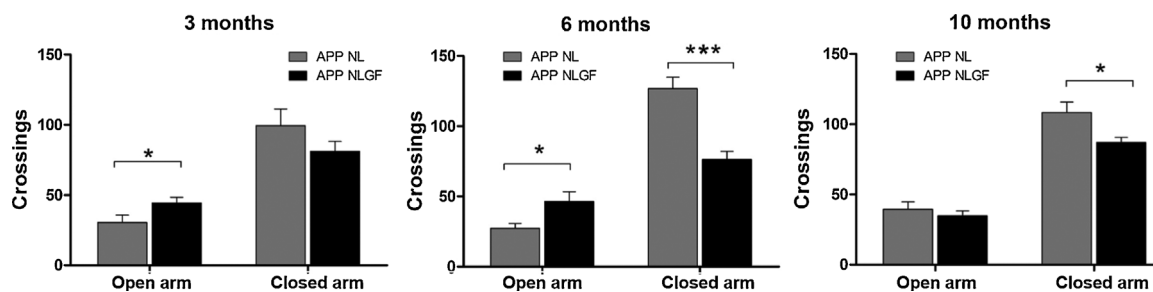


Fig. 3. Anxiety and hyperactivity in the elevated plus maze in APP^{NL-G-F} (black bars) and APP^{NL} mice (grey bars). Left panel: at 3 months, APP^{NL-G-F} mice (n = 8) showed less preference for the close arm than APP^{NL} mice (n = 7); middle panel: preference for the open arm stronger in 6-month-old APP^{NL-G-F} mice (n = 7) compared to APP^{NL} mice (n = 8), with a significant reduction in the preference for the close arm; right panel: 10-month-old APP^{NL-G-F} mice (n = 11) displayed significantly decreased number of beam breaks in the close arm compared to APP^{NL} mice (n = 10). Data are means \pm SEM.

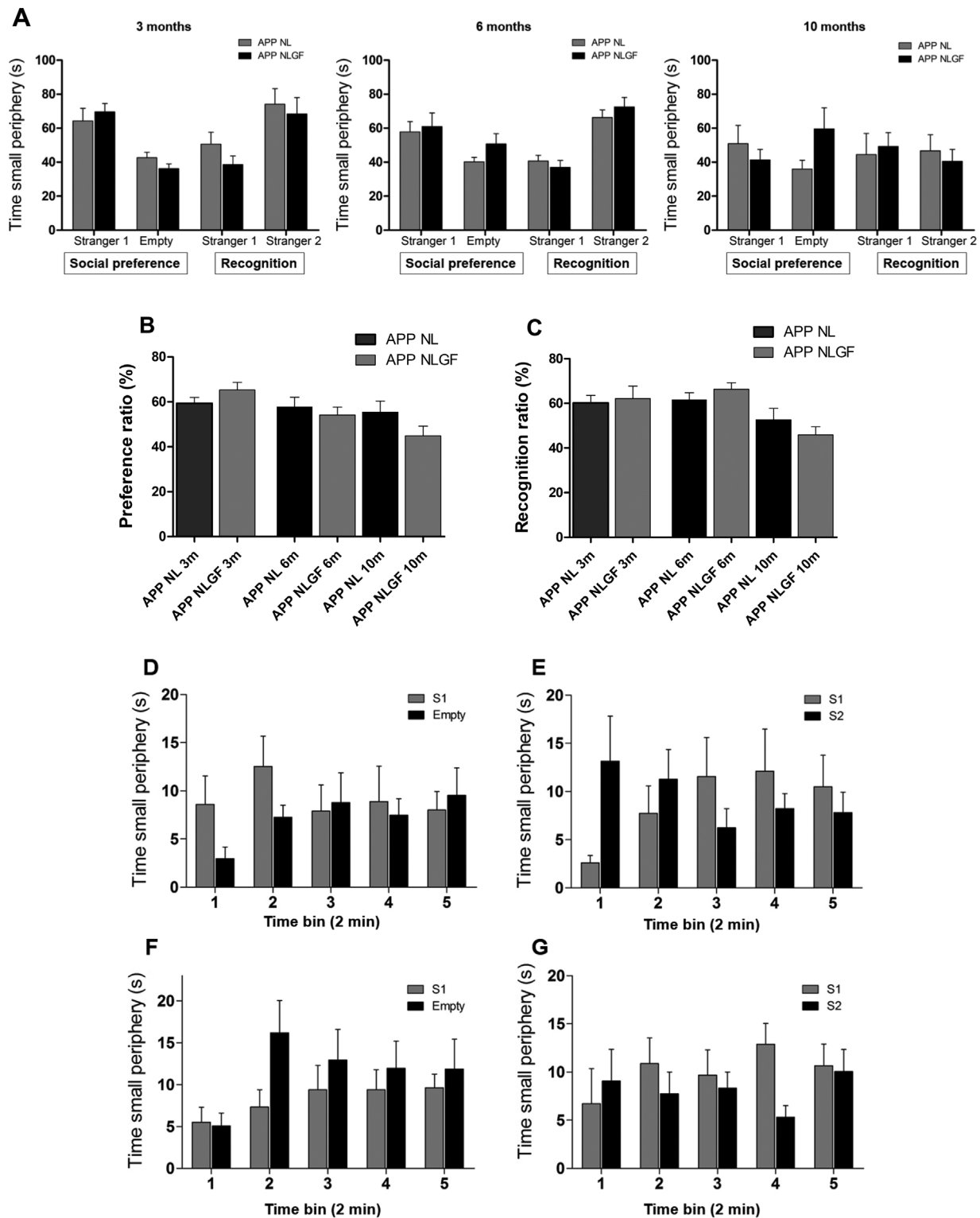


Fig. 4. Social preference in APP^{NL-G-F} and APP^{NL} mice at 3, 6 and 10 months of age. (A) Left panel: at 3 months, both groups showed preference for S1 side over the empty side, but more pronounced preference in APP^{NL-G-F} mice (open bars; $n = 9, 7, 10$ respectively) than APP^{NL} mice (filled bars; $n = 8, 8, 8$, respectively). Increased preference for the novel mouse (S2) in both genotypes during the recognition phase; middle panel: 6-month-old APP^{NL-G-F} mice had little preference towards S1 during the social preference trial, while they explore S2 more than S1 in the recognition phase. Time spent with the novel mouse in the second trial was reduced in APP^{NL} mice compared to APP^{NL-G-F} ; right panel: at 10 months of age, none of the two genotypes displayed any preference for the novel mouse. In fact, APP^{NL-G-F} mice showed preference for the empty side over the S1 during the first trial. (B) During the sociability phase, both groups displayed similar preference ratio at 3 and 6 months, indicating that APP^{NL} ($n = 8$ and $n = 8$, respectively) and APP^{NL-G-F} mice ($n = 9$ and $n = 7$, respectively) displayed similar preference for S1 versus empty cage. A tendency towards reduced preference in APP^{NL-G-F} mice ($n = 10$) starting at 10 months compared to APP^{NL} mice ($n = 8$). (C) The recognition ratio increased at 3, 6 and 10 months in APP^{NL} mice (not significant). Time bin analysis of social preference (D & F) and recognition for novelty (E & G) in APP^{NL} (D & E) and APP^{NL-G-F} mice (F & G) at 10 months of age: (D) APP^{NL} mice showed increased exploration of S1 compared to empty cage only for the first two time bins. (E) APP^{NL} mice had a strong preference for S2 during the beginning of the recognition phase (time bins 1 and 2). (F) APP^{NL-G-F} mice showed equal interest for S1 and empty side during the first time bin with a pronounced increased in exploration of the empty side from the second time bin. (G) APP^{NL-G-F} mice displayed a preference for S1 over the novel mouse, exploring S2 only during time bin 1. Data are means \pm SEM.

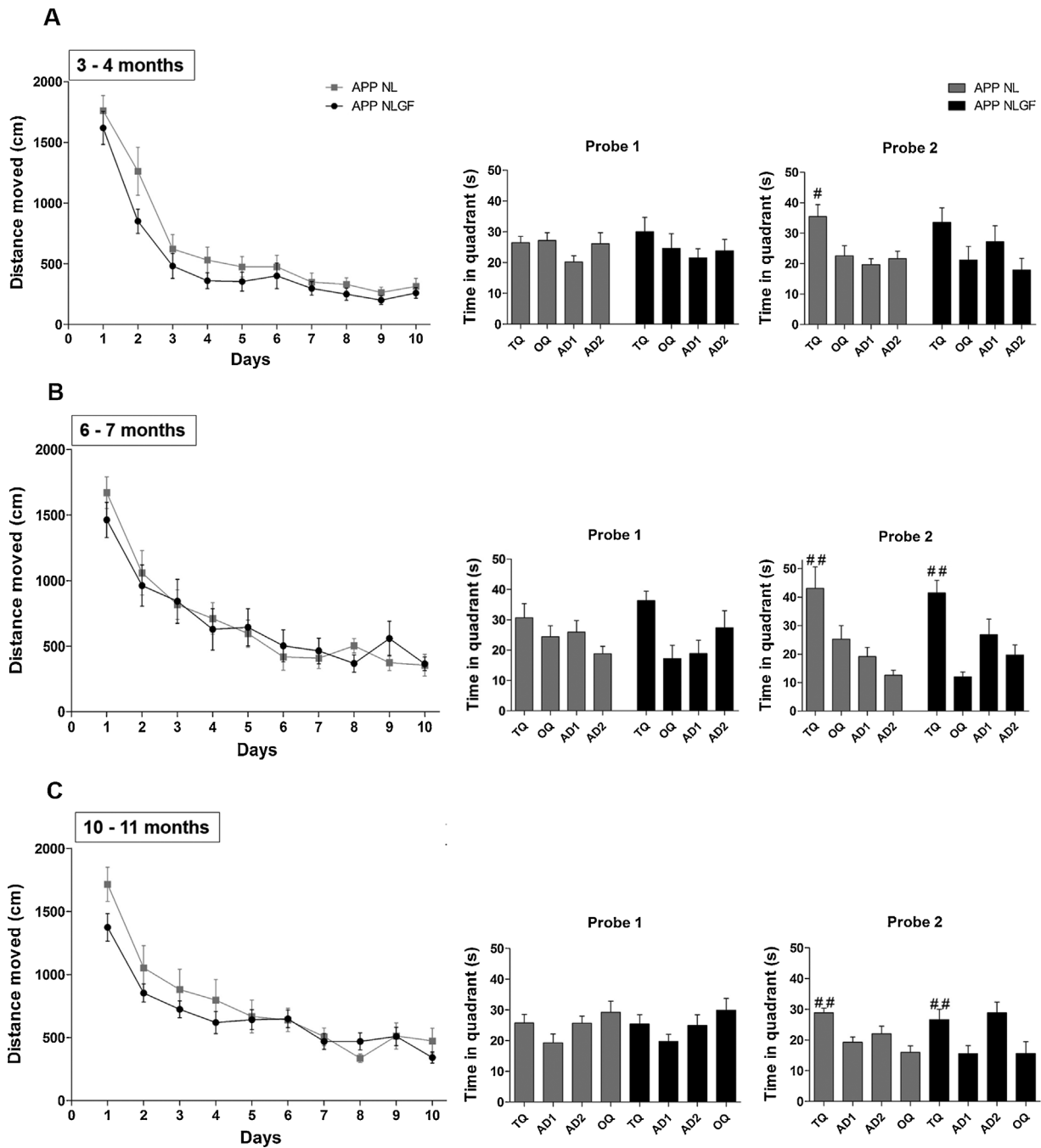


Fig. 5. Morris water maze performance at 3–4, 6–7 and 10–11 months of age in APP^{NL} (grey bars; $n = 13, 7$ and 12 respectively) and APP^{NL-G-F} mice (black bars; $n = 12, 8$ and 11 respectively). TQ = Target quadrant; AD1 = adjacent 1; AD2 = Adjacent 2; OQ = Opposite quadrant. During 10 days of acquisition, mice were given a probe trial on day 6 (probe 1) and 11 (probe 2) for each time point. At 3–4 months of age, APP^{NL} mice performed at a slower rate than APP^{NL-G-F} during the first days of acquisition learning, reaching similar performance on day 6 (A, left panel), the probe trial showed no differences between the two groups (A, middle panel). During probe 2 on day 11 after acquisition learning, memory retention was increased in APP^{NL} compared to APP^{NL-G-F} mice as shown by significant target preference (A, right panel). At 6–7 months, both groups showed good performance during the acquisition of the task (B, left panel). On the first probe trial, although a mild preference for the target quadrant was present, no significant differences were found (B, middle panel). However, a significant increase of time spent in the target quadrant over the other quadrants was detected in both groups (B, right panel). 10–11 months old-APP^{NL} and APP^{NL-G-F} mice learned the platform location (C, left panel) and showed retention memory during probe 2 (C right panel). However, after 5 days of acquisition learning, on day 6 the first probe did not show any indication of preference for the target quadrant in none of the groups (C middle panel). Total distance swam and time spent in quadrant expressed as means \pm SEM. Target quadrant versus opposite quadrant indicated with # $P < 0.05$, ## $P < 0.01$, ### $P < 0.001$ (Tukey pairwise).

quadrant than the other 3 quadrants ($p = 0.007$, $p = 0.002$). At 10–11 months (Fig. 5C), we found very similar patterns of spatial learning and memory performance compared to 6–7 months. Two-way RM-ANOVA showed significant effects of *day* ($F_{9,181} = 31.34$, $p < 0.001$), but no effect of *group* ($F_{1,189} = 0.5625$, $p = 0.4616$) or *group* by *day* ($F_{(9,181)} = 1.461$, $p = 0.1653$) on time spent in the target quadrant. During the second probe, significant preference for the target quadrant

was found in both APP^{NL} ($p = 0.0012$) and APP^{NL-G-F} mice ($p = 0.005$). Swimming velocity was not different between groups (data not shown).

3.5. Spatial reversal learning

Reversal learning was investigated also in MWM by changing the

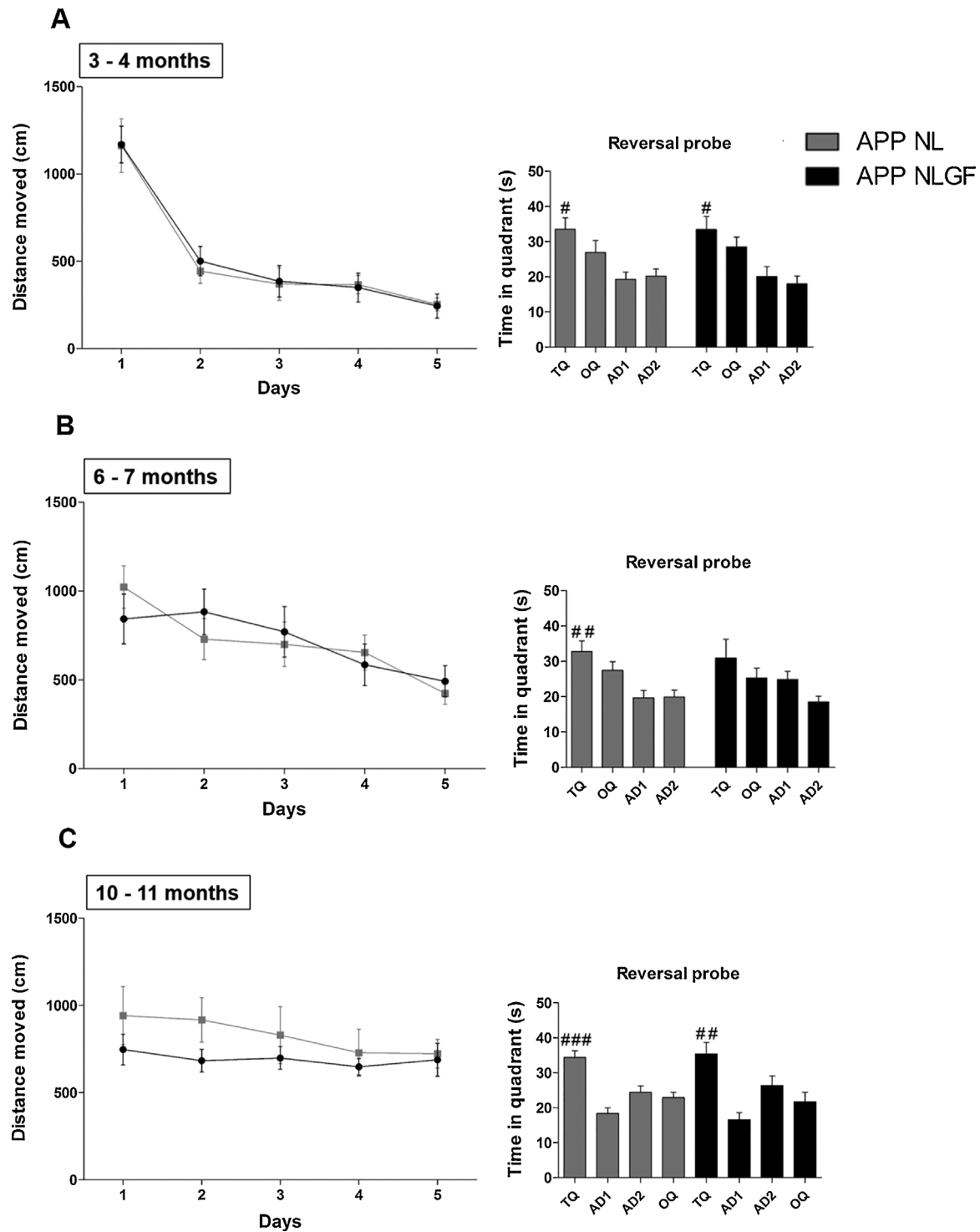


Fig. 6. Water maze reversal learning at 3–4, 6–7 and 10–11 months of age in APP^{NL} (grey bars; $n = 13, 7$ and 12 respectively) and APP^{NL-G-F} mice (black bars; $n = 12, 8$ and 11 respectively). TQ = Target quadrant; AD1 = adjacent 1; AD2 = Adjacent 2; OQ = Opposite quadrant. Total distance swam and time spent in quadrant expressed as means \pm SEM. At 3–4 months, both APP^{NL} and APP^{NL-G-F} mice learned the reversed platform location (A, left panel) and showed good memory retention in the probe test (A, right panel). 6–7 months old- APP^{NL} and APP^{NL-G-F} mice showed similar performance during the acquisition of the new platform location (B, left panel). During the probe test APP^{NL} mice had a significant preference for target quadrant over the other quadrants, whereas APP^{NL-G-F} mice were marginally worse at this (B right panel). At 10–11 months, there was no significant reversal learning curve (C, left panel), but both APP^{NL} and APP^{NL-G-F} mice eventually did display a preference for the new target location (C right panel). Data are means \pm SEM. Target quadrant versus opposite quadrants indicated with # $P < 0.05$, ## $P < 0.01$, ### $P < 0.001$ (Tukey pairwise).

platform position to the opposite quadrant. Studying reversal learning in mice allows the study of cognitive flexibility, which was altered in some other AD models [27]. During the reversal phase of learning at 3–4 months of age (Fig. 6A), APP^{NL} and APP^{NL-G-F} mice perform equally well. RM-ANOVA revealed a main effect of the factor *day* (F

$(4,96) = 51.49$; $p < 0.0001$), and no effect of genotype. The probe trial showed that both APP^{NL} ($p = 0.02$) and APP^{NL-G-F} mice ($p = 0.02$) had a preference for the target quadrant. At 6–7 months of age (Fig. 6B), reversal learning curves show that APP^{NL-G-F} and APP^{NL} learned the new platform location at a similar rate. RM-ANOVA

indicates only main effect of *day* ($F_{4,52} = 5.514$; $p = 0.0009$). During the reversal probe trial, APP^{NL} mice spent more time in the target quadrant than in the other quadrants ($p = 0.007$), whereas APP^{NL-G-F} mice failed to show such a preference ($p = 0.2$). This marginal effect during the reversal retention test could be due to somewhat more variable performance in the APP^{NL-G-F} group, and not necessary to a robust cognitive defect as such. In effect, a previous report failed to show early cognitive defects in these mice [8], and in our report, at 10–11 months of age (Fig. 6C), no differences were observed, neither in reversal learning, nor in probe trial performance. We cannot exclude that more challenging testing might still reveal the robust occurrence of early cognitive changes in these mice.

3.6. Prefrontal network synchrony

We used rsfMRI to compare functional connectivity between APP^{NL-G-F} and APP^{NL} mice in telencephalic regions with an established role in spatial learning and reversal learning. We analyzed rsfMRI data with a seed-based strategy to investigate the synchrony of BOLD signals between specified brain regions. Synchrony of activity between regions connected to PFC was stronger in the APP^{NL-G-F} group than the APP^{NL} group. We analyzed regions with correlated patterns of neuronal activity at 3, 7 and 11 months of age. Seed-based analysis showed increased synchrony at 3 months in the PFC network in APP^{NL-G-F} compared to APP^{NL} mice ($p = 0.007$; Fig. 7B, right panel). This network comprised motor cortex, cingulate/retrosplenial cortex, somatosensory cortex and CA1 region of hippocampus (uncorrected,

$p < 0.001$; Fig. 7). However, we found no differences in PFC network synchrony at 7 and 11 months of age ($p = 0.99$ and $p = 0.85$, respectively; Sidak's multiple comparisons test, 2-way ANOVA; Fig. 7B, right panel).

4. Discussion

Mouse models of AD have been instrumental to investigate pathological mechanisms and pharmacological interventions [27]. In the presently studied APP^{NL-G-F} mouse model, plaque deposition starts early and saturates around 7 months of age. Neuro-inflammation and synaptic alterations, which constitute two other hallmarks of AD pathology, are observed in APP^{NL-G-F} mice as well [7]. APP^{NL-G-F} mice were constructed to control for some of the confounds of other AD mouse models, because the knock-in strategy used to generate this model induces less unwanted artifacts, and the phenotype of APP^{NL-G-F} mice would be more specifically related to AD pathology. At least part of the phenotypes reported in APP transgenic mouse models could be caused by APP overexpression. For example, APP overexpression perturbs axonal transport because APP interacts with kinesin via JIP-1 [7]. Therefore, early behavioral impairments observed in such transgenic mice might be induced by the interaction of overexpressed APP with a variety of molecular substrates, and not by AD pathology proper. However as it turned-out, APP^{NL-G-F} mice appeared to display a relatively mild behavioral phenotype, in accordance with previous reports, which only becomes more manifest at a relatively advanced age [7,8].

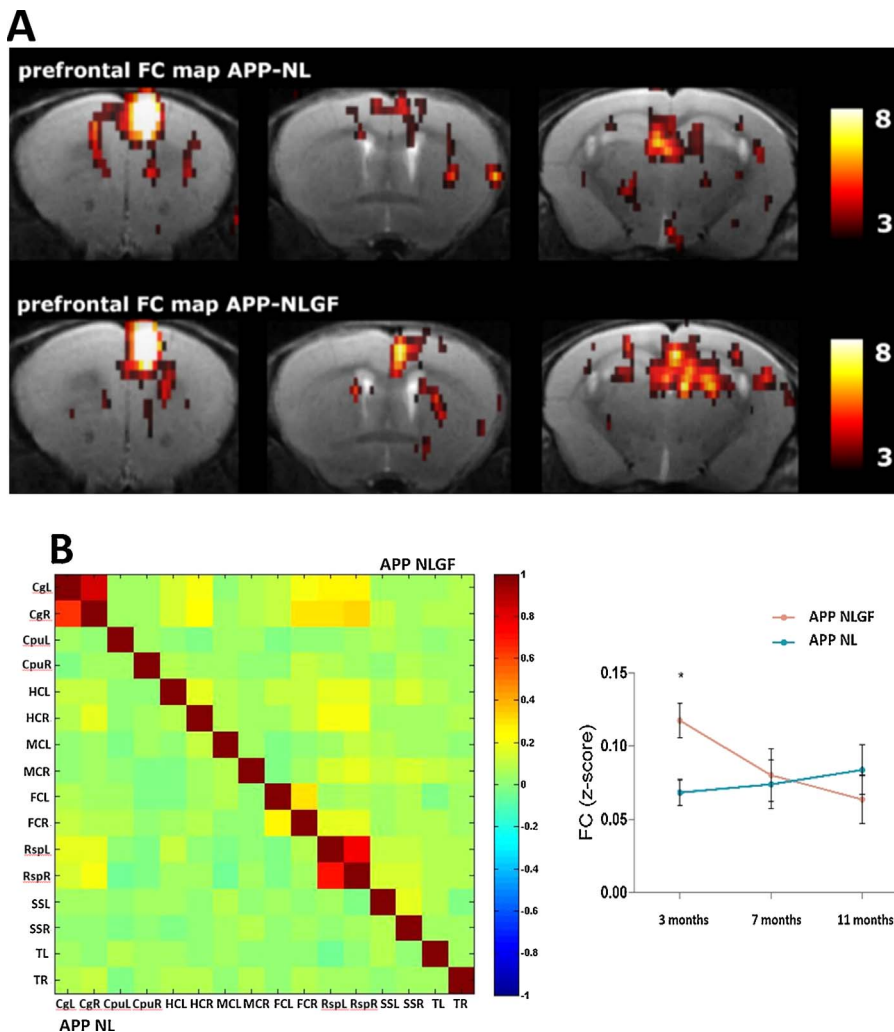


Fig. 7. Increased functional connectivity at 3 months in APP^{NL-G-F} mice. (A) The functional connectivity (FC) map shows increased synchrony in regions that are functionally connected to the prefrontal cortex. (B) Correlation coefficients of paired regions indicate increased prefrontal connectivity in APP^{NL-G-F} mice (left panel, upper part) compared to APP^{NL} (lower part). This hypersynchrony was no longer present at later ages as shown by mean FC at 7 and 11 months of age (right panel).

Using a somewhat more detailed approach, we presently report that APP^{NL-G-F} mice already display some behavioral changes at an early age. Behavioral testing in APP^{NL-G-F} mice was carried out at three different time points to investigate the precise onset of cognitive or behavioral changes, using tests with reported sensitivity to age-related changes in wild-type C57BL/6 mice [29]. We observed increases in nocturnal cage activity in APP^{NL-G-F} mice already at 3 months of age. Increased locomotor activity and disturbances of circadian rhythm and activity have been observed in other AD mouse models [34,35], but Masuda et al. [36] observed impulsivity and enhanced compulsivity only from 6 to 7 months in APP^{NL-G-F} mice. It is important to note that their measures were not directly linked to spontaneous locomotor activity as they included cognitive components that are not investigated in our cage activity test. In our study, mildly increased cage activity was specific to this task and not observed in other tasks.

APP^{NL-G-F} mice displayed reduced anxiety-related behavior in the open field as well as in the elevated plus maze from 3 months of age. The mice also displayed variable changes in social behaviors and memory. The open field test results were also somewhat more variable as 6 months-old APP^{NL-G-F} mice spent more time in the center of the open field, whereas 3- and 10-month-old APP^{NL-G-F} mice spent equal time exploring the center and the periphery. However, it should be noted that open field exploration is indeed reportedly variable, and might be less reliable to measure anxiety [37,38], compared to other anxiety-related tasks [39]. APP^{NL-G-F} mice showed anxiolytic-like behavior in the elevated plus maze, comparable to that of other AD mouse models, which could be attributed to disinhibition resulting from AD pathology [40].

Several genetic mouse models of AD that display amyloid pathology, for example APP/PS1 mice [41], display impairments in spatial-cognitive tasks such as radial-arm water maze or MWM [42]. These tasks are well-established to be hippocampus as well as mPFC dependent [43]. APP^{NL-G-F} and APP^{NL} mice performed very similarly in our MWM acquisition experiments, showing only marginal impairments in the reversal reference memory task at 6 months of age. This subtle defect could be due to somewhat more variable performance, and may not be a cognitive defect as such, which more challenging cognitive testing might reveal. Moreover this change in performance was not observed at later age, possibly overshadowed by the age-related decline in wild-type C57BL/6 mice [44]. Studies in other mouse models of A β accumulation have found more robustly impaired reversal learning [33,45–47], but these studies differ from ours in several ways. The more severe phenotypes mostly occurred in older animals (e.g., 12 months of age), when the pathology is more advanced compared to the early plaque stage in our mice. Also, they used mouse models that overexpress APP, whereas our model exhibits A β amyloidosis without APP overexpression (lacking its potential artifacts). Our mouse model exhibits relatively slow onset of pathology compared to other transgenic models of AD [7], and testing these animals at more advanced ages might reveal more severe behavioral changes (however, testing at such senescent ages could be confounded as well).

Imaging techniques might actually be more sensitive to detect changes in brain function. Indeed, rsfMRI revealed hypersynchronized activity between memory-related areas in our mice, already at 3 months of age. The regions showing increased correlated patterns of neuronal activity were mainly those included in the prefrontal network. It still remains somewhat obscure what this hypersynchronized activity signifies or to which aspect of the pathology it could be related, but present findings are consistent with our previous observation of hypersynchronized activity in another amyloidosis model [48]. It remains difficult to relate hypersynchronous brain activity to behavioral performance, but we have previously shown that increased cortical connectivity coincides with impaired reversal learning in PFC-lesioned mice [26].

The observed changes that occur before prominent plaque deposition could be attributed to the neurotoxic effects of soluble A β , rather

than actual A β plaques that mostly occur later [48]. The present report makes this even more likely as the knock-in model does not display any artifacts of APP overexpression. A previous study showed a reduction of mushroom spines at relatively early age in these mice [49], but they do not display any tau pathology or cell death, suggesting that the observed functional changes are entirely due to A β -induced effects. Thus, the observed rsfMRI changes could be an early sign of pathology, but we cannot exclude that the hypersynchronous frontal network could also be a neurobehavioral response to compensate for A β -induced dysfunction.

Acknowledgements

This research was financially supported by the federal science fund FWO-Vlaanderen (G058714 and GOD76114). The authors wish to thank Dr. Stijn Stroobants for his help with the behavioral analyses.

References

- [1] G.G. Glenner, C.W. Wong, Alzheimer's disease: initial report of the purification and characterization of a novel cerebrovascular amyloid protein, *Biochem. Biophys. Res. Commun.* 120 (1984) 885–890.
- [2] J. Hardy, D.J. Selkoe, The amyloid hypothesis of Alzheimer's disease: progress and problems on the road to therapeutics, *Science* 297 (2002) 353–356.
- [3] C.L. Masters, G. Multhaup, G. Simms, J. Pottgiesser, R.N. Martins, K. Beyreuther, Neuronal origin of a cerebral amyloid: neurofibrillary tangles of Alzheimer's disease contain the same protein as the amyloid of plaque cores and blood vessels, *EMBO J.* 4 (1985) 2757–2763.
- [4] I. Grundke-Iqbal, K. Iqbal, Y.C. Tung, M. Quinlan, H.M. Wisniewski, L.I. Binder, Abnormal phosphorylation of the microtubule-associated protein tau (τ) in Alzheimer cytoskeletal pathology, *Proc. Natl. Acad. Sci. U. S. A.* 83 (1986) 4913–4917.
- [5] K. Hsiao, P. Chapman, S. Nilsen, C. Eckman, Y. Harigaya, S. Younkin, et al., Correlative memory deficits Ab elevation, and amyloid plaques in transgenic mice, *Science* 274 (1996) 99–103.
- [6] C. Sturchler-Pierrat, D. Abramowski, M. Duke, K.H. Wiederhold, C. Mistl, S. Rothacher, et al., Two amyloid precursor protein transgenic mouse models with Alzheimer disease-like pathology, *Proc. Natl. Acad. Sci. U. S. A.* 94 (1997) 13287–13292.
- [7] T. Saito, Y. Matsuba, N. Mihira, J. Takano, P. Nilsson, S. Itoharu, et al., Single APP knock-in mouse models of Alzheimer's disease, *Nat. Neurosci.* 17 (2014) 661–663.
- [8] L.S. Whyte, K.M. Hemsley, A.A. Lau, S. Hassiotis, T. Saito, T.C. Saido, J.J. Hopwood, T.J. Sargeant, Reduction in open field activity in the absence of memory deficits in the APP^{NL-G-F} knock-in mouse model of Alzheimer's disease, *Behav. Brain Res.* 336 (2018) 177–181.
- [9] H. Amieva, S. Lafont, I. Rouch-Leroyer, C. Rainville, J.-F. Dartigues, J.-M. Orgogozo, et al., Evidencing inhibitory deficits in Alzheimer's disease through interference effects and shifting disabilities in the Stroop test, *Arch. Clin. Neuropsychol.* 19 (2004) 791–803.
- [10] J. Lindeboom, H. Weinstein, Neuropsychology of cognitive ageing, minimal cognitive impairment Alzheimer's disease, and vascular cognitive impairment, *Eur. J. Pharmacol.* 490 (2004) 83–86.
- [11] R. Ossenkoppele, B.I. Cohn-Sheehy, R. La Joie, J.W. Vogel, C. Möller, M. Lehmann, et al., Atrophy patterns in early clinical stages across distinct phenotypes of Alzheimer's disease, *Human Brain Mapp.* 36 (2015) 4421–4437.
- [12] J. Calderon, Perception, attention, and working memory are disproportionately impaired in dementia with Lewy bodies compared with Alzheimer's disease, *J. Neurol. Neurosurg. Psychiatry* 70 (2001) 157–164.
- [13] G.B. Bissonette, E.M. Powell, Reversal learning and attentional set-shifting in mice, *Neuropharmacology* 62 (2012) 1168–1174.
- [14] M. Binnewijzend, S.M. Adriaanse, W.M. van der Flier, C.E. Teunissen, J.C. de Munck, C.J. Stam, et al., Brain network alterations in Alzheimer's disease measured by Eigenvector centrality in fMRI are related to cognition and CSF biomarkers, *Human Brain Mapp.* 35 (2014) 2383–2393.
- [15] M. Binnewijzend, M.M. Schoonheim, E. Sanz-Arigita, A.M. Wink, W.M. van der Flier, N. Tolboom, et al., Resting-state fMRI changes in Alzheimer's disease and mild cognitive impairment, *Neurobiol. Aging* 33 (2012) 2018–2028.
- [16] J.L. Cummings, S.J. Banks, R.K. Gary, J.W. Kinney, J.M. Lombardo, R.R. Walsh, et al., Alzheimer's disease drug development: translational neuroscience strategies, *CNS Spectr.* 18 (2013) 128–138.
- [17] E. Jonckers, J. Van Audekerke, G. De Visscher, A. Van der Linden, M. Verhoye, Functional connectivity fMRI of the rodent brain: comparison of functional connectivity networks in rat and mouse, *PLoS One* 6 (2011) e18876.
- [18] A.J. Schwarz, N. Gass, A. Sartorius, L. Zheng, M. Spedding, E. Schenker, et al., The low-frequency blood oxygenation level-dependent functional connectivity signature of the hippocampal-prefrontal network in the rat brain, *Neuroscience* 228 (2013) 243–258.
- [19] M.P. van den Heuvel, H.E. Hulshoff Pol, Exploring the brain network: a review on resting-state fMRI functional connectivity, *Eur. Neuropsychopharmacol.* 20 (2010) 519–534.

- [20] J.S. Damoiseaux, C.F. Beckmann, E.J.S. Arigita, F. Barkhof, P. Scheltens, C.J. Stam, et al., Reduced resting-state brain activity in the default network in normal aging, *Cereb. Cortex* 18 (2008) 1856–1864.
- [21] D. Shah, E. Jonckers, J. Praet, G. Vanhoutte, Y. Delgado, R. Palacios, C. Bigot, et al., Resting state fMRI reveals diminished functional connectivity in a mouse model of amyloidosis, *PLoS One* 8 (2013) e84241.
- [22] A. Van der Jeugd, H. Goddyn, A. Laeremans, L. Arckens, R. D’Hooge, T. Verguts, Hippocampal involvement in the acquisition of relational associations: but not in the expression of a transitive inference task in mice, *Behav. Neurosci.* 123 (2009) 109–114.
- [23] A. Naert, Z. Callaerts-Vegh, D. Moechars, T. Meert, R. D’Hooge, Vglut2 haploinsufficiency enhances behavioral sensitivity to MK-801 and amphetamine in mice, *Prog. Neuropsychopharmacol. Biol. Psychiatry* 35 (2011) 1316–1321.
- [24] R. Morris, Developments of a water-maze procedure for studying spatial learning in the rat, *J. Neurosci. Methods* 11 (1984) 47–60.
- [25] R. D’Hooge, P.P. De Deyn, Applications of the Morris water maze in the study of learning and memory, *Brain Res. Rev.* 36 (2001) 60–90.
- [26] A. Latif-Hernandez, D. Shah, T. Ahmed, A.C. Lo, Z. Callaerts-Vegh, A. Van der Linden, et al., Quinolinic acid injection in mouse medial prefrontal cortex affects reversal learning abilities, cortical connectivity and hippocampal synaptic plasticity, *Sci. Rep.* 6 (2016) 36489.
- [27] S.J. Webster, A.D. Bachstetter, P.T. Nelson, F. Schmitt, L.J. Van Eldik, Using mice to model Alzheimer’s dementia: an overview of the clinical disease and the preclinical behavioral changes in 10 mouse models, *Front. Genet.* 5 (2014) 88.
- [28] R. Lalonde, M. Dumont, M. Staufienbiel, C. Sturchler-Pierrat, C. Strazielle, Spatial learning exploration, anxiety, and motor coordination in female APP23 transgenic mice with the Swedish mutation, *Brain Res.* 956 (2002) 36–44.
- [29] H. Shoji, K. Takao, S. Hattori, T. Miyakawa, Age-related changes in behavior in C57BL/6J mice from young adulthood to middle age, *Mol. Brain* 9 (2016) 11.
- [30] A.C. Lo, Z. Callaerts-Vegh, A.F. Nunes, C.M.P. Rodrigues, R. D’Hooge, Tauroursodeoxycholic acid (TUDCA) supplementation prevents cognitive impairment and amyloid deposition in APP/PS1 mice, *Neurobiol. Dis.* 50 (2013) 21–29.
- [31] Y.-H. Hsiao, H.-C. Hung, S.-H. Chen, P.-W. Gean, Social interaction rescues memory deficit in an animal model of Alzheimer’s disease by increasing BDNF-dependent hippocampal neurogenesis, *J. Neurosci.* 34 (2014) 16207–16219.
- [32] Z. Callaerts-Vegh, S. Leo, B. Vermaercke, T. Meert, R. D’Hooge, LPA(5) receptor plays a role in pain sensitivity: emotional exploration and reversal learning, *Genes Brain Behav.* 11 (2012) 1009–1019.
- [33] P. Papadopoulos, P. Rosa-Neto, J. Rochford, E. Hamel, Pioglitazone improves reversal learning and exerts mixed cerebrovascular effects in a mouse model of Alzheimer’s disease with combined amyloid- β and cerebrovascular pathology, *PLoS One* 8 (2013) e68612.
- [34] S. Pietropaolo, J. Feldon, B.K. Yee, Age-dependent phenotypic characteristics of a triple transgenic mouse model of Alzheimer disease, *Behav. Neurosci.* 122 (2008) 733–747.
- [35] R. Sterniczuk, R.H. Dyck, F.M. LaFerla, M.C. Antle, Characterization of the 3xTg-AD mouse model of Alzheimer’s disease: part 1. Circadian changes, *Brain Res* 1348 (2010) 139–148.
- [36] A. Masuda, Y. Kobayashi, N. Kogo, T. Saito, T.C. Saido, S. Itoharu, Cognitive deficits in single app knock-in mouse models, *Neurobiol. Learn Mem.* 135 (2016) 73–82.
- [37] Z. Callaerts-Vegh, T. Beckers, S.M. Ball, F. Baeyens, P.F. Callaerts, J.F. Cryan, R. D’Hooge, Concomitant deficits in working memory and fear extinction are functionally dissociated from reduced anxiety in metabotropic glutamate receptor 7-deficient mice, *J. Neurosci.* 26 (2006) 6573–6582.
- [38] H. Goddyn, S. Leo, T. Meert, R. D’Hooge, Differences in behavioural test battery performance between mice with hippocampal and cerebellar lesions, *Behav. Brain Res.* 173 (2006) 138–147.
- [39] M.M. van Gaalen, T. Steckler, Behavioural analysis of four mouse strains in an anxiety test battery, *Behav. Brain Res.* 115 (2000) 95–106.
- [40] E. Ognibene, S. Middei, S. Daniele, W. Adriani, O. Ghirardi, A. Caprioli, et al., Aspects of spatial memory and behavioral disinhibition in Tg2576 transgenic mice as a model of Alzheimer’s disease, *Behav. Brain Res.* 156 (2005) 225–232.
- [41] S.J. Kempf, A. Metaxas, M. Ibáñez-Vea, S. Darvesh, B. Finsen, M.R. Larsen, An integrated proteomics approach shows synaptic plasticity changes in an APP/PS1 Alzheimer’s mouse model, *Oncotarget* 7 (2014) 33627–33648.
- [42] Y. Ding, A. Qiao, Z. Wang, J.S. Goodwin, E.-S. Lee, M.L. Block, et al., Retinoic acid attenuates – amyloid deposition and rescues memory deficits in an Alzheimer’s disease transgenic mouse model, *J. Neurosci.* 28 (2008) 11622–11634.
- [43] D.G. Woolley, A. Laeremans, I. Gantois, D. Mantini, B. Vermaercke, H.P. Op de Beeck, N. Wenderoth, L. Arckens, R. D’Hooge, Homologous involvement of striatum and prefrontal cortex in rodent and human water maze learning, *Proc. Natl. Acad. Sci. U. S. A.* 110 (2013) 3131–3136.
- [44] J. Kennard, Age sensitivity of behavioral tests and brain substrates of normal aging in mice, *Front. Aging Neurosci.* (2011) 3.
- [45] D. Cheng, J.K. Low, W. Logge, B. Garner, T. Karl, Novel behavioural characteristics of female APPSwe/PS1 Δ E9 double transgenic mice, *Behav. Brain Res.* 260 (2014) 111–118.
- [46] M. Filali, R. Lalonde, Age-related cognitive decline and nesting behavior in an APPSwe/PS1 bigenic model of Alzheimer’s disease, *Brain Res.* 1292 (2009) 93–99.
- [47] J.-M. Zhuo, S.L. Prescott, M.E. Murray, H.-Y. Zhang, M.G. Baxter, M.M. Nicolle, Early discrimination reversal learning impairment and preserved spatial learning in a longitudinal study of Tg2576 APPsw mice, *Neurobiol. Aging* 28 (2007) 1248–1257.
- [48] D. Shah, J. Praet, A. Latif Hernandez, C. Höfling, C. Anckaerts, F. Bard, et al., Early pathologic amyloid induces hypersynchrony of BOLD resting-state networks in transgenic mice and provides an early therapeutic window before amyloid plaque deposition, *Alzheimers Dement.* 12 (2016) 964–976.
- [49] H. Zhang, L. Wu, E. Pchitskaya, O. Zakharova, T. Saito, T. Saido, et al., Neuronal store-operated calcium entry and mushroom spine loss in amyloid precursor protein knock-in mouse model of Alzheimer’s disease, *J. Neurosci.* 35 (2015) 13275–13286.